# Biomechanical and Energetic Consequences of Stride Length–Frequency Modulation across Running Speeds

***Mandira Bhowmik[1], Md Mostafizur Rahman[2]**

**[1]Department of Biomedical Engineering, University of Arizona, Tucson, Arizona, USA**

**[2]Dhaka University of Engineering & Technology, Gazipur, Bangladesh**

***Corresponding Author**

**DOI: https://doi.org/10.51584/IJRIAS.2026.11070051**

**Received: 20 July 2026; Accepted: 25 July 2026; Published: 31 July 2026**

## ABSTRACT

Running speed is governed by coordinated adaptations in stride mechanics and center-of-mass (CoM) dynamics, and this study examined speed-dependent changes in stride parameters, CoM kinematics, and mechanical energy during slow and fast running using two-dimensional kinematic approach and computational modeling. A physically trained adult performed self-selected slow and fast running trials, with hip marker trajectories used as a surrogate for CoM motion. Slow running was characterized by a lower stride frequency (≈ 0.8 Hz), larger vertical CoM displacement (≈ 0.20 m), and greater gravitational potential energy fluctuations (≈ 140 J), accompanied by modest vertical velocity peaks (≈ 0.9 m/s upward and −0.5 m/s downward), indicating lower propulsive and impact demands. In contrast, fast running exhibited a substantially higher stride frequency (≈ 2.67 Hz), reduced vertical CoM oscillation (≈ 0.10 m), and smaller potential energy fluctuations (≈ 70 J), while vertical velocity magnitudes increased markedly (≈ 1.2 to 1.3 m/s upward and −1.1 m/s downward), reflecting elevated mechanical power output and greater impact loading. Total mechanical energy profiles further demonstrated smoother, lower-amplitude fluctuations during slow running and larger, more variable kinetic energy peaks during fast running, consistent with increased reliance on elastic energy storage and return at higher speeds. Collectively, these findings indicate a speed-dependent transition from an economical, low-impact gait strategy at slower speeds to a spring-mass-dominated, high-power locomotor pattern at faster speeds, highlighting the dynamic interplay between stride length, stride frequency, and CoM energy regulation in human running.

**Keywords:** Stride length–frequency interaction; center of mass kinematics; vertical and horizontal kinetic energy; gait speed modulation; 2D video-based motion analysis.

## INTRODUCTION

Human locomotion, particularly running, is governed by complex biomechanical processes involving the coordinated interaction of muscular forces, energy transformations, and stride dynamics. During running, mechanical work is continuously performed to raise and accelerate the body's center of mass, while elastic structures within the musculoskeletal system store and return energy, thereby enhancing movement efficiency. An analysis of these processes is essential for improving athletic performance, reducing metabolic cost, and minimizing the risk of musculoskeletal injury.

Early experimental investigations laid the foundation for modern locomotion biomechanics. Krebbekx et al. (2025) provided one of the first quantitative analyses of vertical body movements and energy expenditure during locomotion. Subsequent landmark studies demonstrated that during running, kinetic and potential energy variations occur largely in phase, allowing partial mechanical energy recovery through elastic recoil mechanisms (Luciano et al., 2024; Baček et al., 2024). These findings established the concept that running efficiency that is strongly influenced by the exchange and recovery of mechanical energy within each gait cycle. The mechanical work associated with velocity changes and gravitational displacement, emphasizing the

energetic consequences of speed modulation during running was analyzed further by Jiang et al. (2024). Arellano & Kram (2014) extended this work by showing that the energy cost of running per unit distance remains approximately constant across a wide range of speeds on level ground, while being significantly affected by slope. Usherwood (2024) contributed a mechanical perspective by describing the forces and moments acting at the joints during walking and running, offering a framework for analyzing muscular contributions to locomotion. More recent investigations have expanded the scope of locomotion research to include environmental and neuromuscular factors. Orr et al. (2022) explored human locomotion under sub-gravity conditions, highlighting the role of gravitational acceleration in shaping stride mechanics and energy expenditure. Contemporary studies, such as those by Arellano and Vega (2024), have emphasized the importance of inter limb coordination and neural coupling between the arms and legs, particularly in the context of gait rehabilitation and movement efficiency.

Despite the extensive analyses of literature on running biomechanics, much of the existing research focuses on isolated components of locomotion, such as external mechanical work, metabolic energy cost, or elastic energy recovery. While these studies have yielded valuable insights, they often lack an integrated perspective that simultaneously considers stride parameters, mechanical energy transformations, and speed-dependent adaptations. In particular, the interaction between stride length, stride frequency, and energy expenditure across different running speeds remains insufficiently explored within a unified biomechanical framework. It is well known that how these parameters co-evolve is critical for identifying optimal running strategies, improving performance, and mitigating repetitive loading that may contribute to overuse injuries. The increasing availability of high-resolution motion capture systems and advanced computational tools presents an opportunity to revisit classical biomechanical questions with greater precision and integration.

The observed coupling between stride parameters and shock attenuation is consistent with both classical and modern interpretations of running energetics. The findings of Mercer et al. (2002) demonstrate that increases in running velocity are primarily achieved through simultaneous increases in stride length and stride frequency, with stride length exhibiting a stronger relationship with shock attenuation. Furthermore, the work of Cavagna et al. (2002) on external mechanical work and energy exchange indicates that greater stride lengths disrupt the ideal pendulum-like exchange between kinetic and potential energy, increasing reliance on active work and enhancing impact forces that must be attenuated by the musculoskeletal system. The stronger correlation between stride length and shock attenuation reported by Mercer et al. therefore supports the interpretation that stride length is the primary determinant governing both mechanical work generation and impact energy dissipation, while stride frequency plays a secondary role. Collectively, these findings reinforce the unified view that running energetics and shock attenuation are governed by center-of-mass dynamics, with stride length acting as the dominant control variable linking mechanical work and energy expenditure.

However, the novelty of the present study lies in its holistic integration of stride dynamics, mechanical energy analysis, and speed-dependent running mechanics. Unlike previous studies that examined these factors independently, this work synthesizes kinematic, energetic, and temporal parameters within a single analytical framework. By combining two-dimensional motion capture data with computational modeling, this study quantifies kinetic and potential energy fluctuations alongside stride length and frequency across multiple running speeds. Furthermore, this research explicitly builds upon and unifies insights from more than two decades of foundational locomotion studies (Krebbekx et al. (2025); Mercer et al. (2003), Mercer et al. (2002), Mero et al., (1992), while incorporating modern perspectives on neuromuscular coordination (Arellano & Vega, 2024). This integrative approach enables a more comprehensive understanding of how mechanical energy is generated, stored, and recovered during running.

This study presents an integrated biomechanical–computational framework that combines motion-capture-derived kinematics with mechanical energy modeling to quantify speed-dependent locomotor efficiency, offering a low-cost and scalable alternative to force-plate-based systems. While substantial progress has been made in running biomechanics, opportunities remain for more comprehensive analyses that integrate stride dynamics with mechanical energy transformations across different running speeds. Importantly, the contribution of this study does not lie in identifying isolated relationships among these variables, which have been previously explored, but rather in examining their simultaneous interaction within a unified analytical framework, particularly through the coupling of stride parameters and shock attenuation.

ISSN No. 2454-6194 | DOI: 10.51584/IJRIAS |Volume XI Issue VII July 2026

Existing literature has largely focused on individual components of locomotion, such as external mechanical work, metabolic energy expenditure, or muscle efficiency, without fully integrating these elements into a cohesive biomechanical model. In addition, relatively limited attention has been given to how stride parameters—specifically stride length and stride frequency—systematically adapt with running speed and how these adaptations collectively influence impulse generation, mechanical work, power output, and potential injury-related loading. This lack of integrative analysis limits the translational application of biomechanical research for optimizing performance and informing strategies for overuse injury prevention.

This study develops an integrated biomechanical framework that combines a two-dimensional (2D) sagittal-plane kinematic approach with MATLAB-based computational modeling to quantify stride dynamics and mechanical energy exchanges during slow and fast running. Stride length, stride frequency, and segmental accelerations are used to derive kinetic, gravitational potential, and elastic energy components, allowing systematic evaluation of how mechanical work, energy distribution, and shock attenuation vary with running speed. These variables are compared across slow and fast running conditions to characterize speed-dependent adaptations in locomotor efficiency and power generation. Although stride mechanics and energetic measures have been widely studied, they are often analyzed separately, limiting integrated interpretation of running mechanics. Therefore, we hypothesize that both stride length and stride frequency increase with speed, that stride length shows a stronger association with impact-related variables, and that mechanical energy distribution shifts systematically across gait cycles with increasing speed.

**Experimental Setup and procedure**

**Setup:**

The experimental setup shown in Fig. 1 was designed to investigate running biomechanics, with particular emphasis on stride dynamics, mechanical work, and mechanical energy transformations across different running speeds. Recent advances in high-resolution motion capture systems have significantly enhanced the ability to quantify human gait mechanics with high spatial accuracy. However, such systems are often expensive and require controlled laboratory environments, which limits their accessibility and practical use in field-based or resource-constrained settings. Therefore, a simplified two-dimensional (2D) video-based kinematic approach was adopted in this study, which is widely used for the analysis of fundamental gait parameters. This approach provides sufficient accuracy for the evaluation of sagittal-plane variables, particularly stride length and stride frequency, which are the primary focus of the present work. Accordingly, the selected methodology offers a practical and reliable means of capturing essential running mechanics while maintaining experimental feasibility and consistency under controlled treadmill conditions.

Figure 1. A 21-year-old athletic male running.

ISSN No. 2454-6194 | DOI: 10.51584/IJRIAS |Volume XI Issue VII July 2026

The 2D video-based kinematic analysis was conducted using a high-speed camera (240 frames/s), positioned perpendicular to the sagittal plane of motion. The camera was mounted at approximately hip height and placed at a distance of ~3.0 m (10 ft) from the running path to minimize parallax distortion and to ensure full-body visibility throughout the gait cycle. The optical axis of the camera was aligned orthogonally to the direction of motion to preserve geometric fidelity in the recorded kinematic data. Spatial calibration was performed using a calibration line fitted with high-contrast markers placed at uniform 10 cm intervals. The calibration markers were rigidly fixed within the field of view and clearly visible in all recorded trials, enabling accurate conversion from pixel coordinates to real-world dimensions. A single healthy, athletic male participant (age: 21 years; height: 175 cm; body mass: 71 kg) volunteered for the study. The participant was free from musculoskeletal injuries and regularly engaged in athletic activities. The relatively low body fat percentage facilitated clear visualization of anatomical landmarks and minimized soft-tissue artifact during motion tracking. High-contrast reflective markers were attached to key anatomical landmarks to enable kinematic analysis. A marker placed at the greater trochanter region was used as a proxy for the body's center of mass (CoM) to track vertical and horizontal displacement, velocity, and acceleration. An additional marker placed on the foot was used to extract stride-level parameters, including stride length, stride frequency, and running velocity. Prior to data collection, the participant performed a standardized warm-up protocol consisting of dynamic stretching and light jogging to reduce injury risk and ensure consistent neuromuscular performance across trials. All running trials were conducted along a straight path under controlled laboratory conditions.

**Procedure:**

The experiment was conducted in a controlled indoor environment to minimize external influences such as wind resistance and surface irregularities, thereby ensuring reliable and precise data collection. A single 21-year-old male participant with an athletic build (height: 175 cm, mass: 71 kg) was selected to maintain consistency across trials. A vertical calibration line measuring precisely 307.54 cm was positioned parallel to the running path and marked at 10 cm intervals. This reference was used to convert pixel-based measurements from video recordings into real-world dimensions. High-contrast reflective markers were placed on key anatomical landmarks, including the hip and foot, to track the center of mass (CoM) and determine stride parameters such as length, frequency, and velocity.

The participant completed two running trials at distinct speeds: slow running (~3.33 m/s) and fast running (~4.56 m/s). Fast running was characterized by greater CoM vertical displacement, higher vertical and horizontal velocities, larger braking and propulsive phases, longer and more distinct flight phase and slow running was characterized by reduced vertical oscillation, lower forces and velocities, shorter, more stable gait cycle. Motion was captured using a high-speed camera operating at 240 frames per second, positioned perpendicular to the plane of motion at hip height and approximately 3 m (10 ft) from the running path to minimize parallax error. High-speed video data were recorded at a sampling frequency of 240 Hz and exported in uncompressed format for post-processing. All kinematic analyses were performed using custom-written scripts in MATLAB (Math-Works, Natick, MA, USA). Video frames were first converted to gray scale to enhance marker contrast, and marker trajectories were digitized semi-automatically using intensity-based thresholding and centroid detection algorithms.

Filtered displacement data were numerically differentiated using a central difference scheme to obtain velocity and acceleration profiles of the CoM. Vertical and horizontal velocity components were subsequently used to compute kinetic energy, while vertical displacement was used to estimate gravitational potential energy. Elastic energy exchange was inferred from the temporal coupling between kinetic and potential energy fluctuations across the gait cycle. Stride parameters, including stride length and stride frequency, were extracted from periodic foot marker trajectories using peak detection algorithms. Stride-level impulse was estimated by integrating the CoM acceleration over the stance phase, while mechanical work and instantaneous mechanical power were computed from the product of ground reaction force proxies and CoM velocity. All computed variables were segmented into individual gait cycles and averaged across strides for each running condition. Slow and fast running trials were compared using engineered performance indicators, including peak mechanical power, mechanical efficiency, and energy recovery ratio. Data quality was verified through repeatability checks and sensitivity analysis of filtering parameters.

ISSN No. 2454-6194 | DOI: 10.51584/IJRIAS |Volume XI Issue VII July 2026

# RESULTS AND ANALYSIS

### Stride Length-Frequency Interaction across Running Speeds

Running speed in this study was governed by the dynamic interaction between stride length and stride frequency, which together determine how effectively muscular effort is translated into forward motion. In a physically fit young adult (21 years; 165 cm; 71 kg) with regular resistance training and low body fat, this interaction reflects coordinated biomechanical, neuromuscular, and physiological adaptations. At low to moderate speeds, increases in velocity were achieved primarily through stride lengthening, allowing greater horizontal displacement per step with minimal additional metabolic cost. Efficient joint mobility and elastic energy storage in the muscle–tendon units supported smooth and economical movement. As speed increased, reliance on stride length alone became less effective, and stride frequency (cadence) played a progressively greater role. Higher cadence reduced ground contact time and braking forces, requiring enhanced neuromuscular coordination and cardiovascular capacity. At near-maximal speeds, optimal performance resulted from a balanced increase in both stride length and frequency, maximizing propulsion while maintaining stability. This transition reflects a shift from elastic energy utilization to rapid force production and limb cycling, enabling efficient, high-speed locomotion.

Slow running was defined as treadmill running at 50–70% of maximal speed, characterized by longer ground contact time, lower stride frequency, and relatively stable mechanical energy fluctuations, representing submaximal, energy-efficient locomotion. Fast running was defined as 80–100% of maximal speed, characterized by shorter ground contact time, higher stride frequency, and greater mechanical energy fluctuations associated with high-intensity effort. Sagittal-plane kinematics were captured using a fixed lateral camera and analyzed with Kinovea, where anatomical landmarks were tracked frame-by-frame to obtain stride length and stride frequency. Spatial and temporal calibration enabled accurate measurement of displacement and timing variables. A basic stopwatch method was used to estimate stride frequency by counting steps over a fixed time interval, providing a practical cross-check for temporal measurements. Together, these methods ensured reliable assessment of stride dynamics under controlled treadmill conditions.

Running gait parameters obtained using the Basic Stopwatch method and the Kinovea 2D motion capture method at slow and fast speeds are presented in Table 1. Running speed increased from 3.33 m/s to 4.56 m/s, accompanied by increases in both stride frequency and stride length across methods. Stopwatch measurements showed stride frequency increasing from 1.98 to 2.40 strides/s and stride length from 1.71 to 1.90 m, while Kinovea measurements increased from 1.90 to 2.47 strides/s and 1.75 to 1.85 m, respectively. Percentage error (using Kinovea as reference) remained below 5% for all conditions.

These findings confirm that speed is achieved through combined modulation of stride length and frequency. The stopwatch method provided reasonable estimates but showed slightly higher error, particularly at lower speeds, likely due to human reaction-time limitations. In contrast, Kinovea's frame-by-frame analysis enabled more precise detection of gait events, improving sensitivity and consistency. Overall, while the stopwatch method is practical, Kinovea offers superior accuracy for detailed biomechanical analysis.

Table 1. Data collected for Basic Stopwatch and Kinovea 2D Motion Capture methods

| | | **Speed (m/sec)** | **Stride Frequency (stride/sec)** | **Stride Length (m)** |
|---|---|---|---|---|
| Basic Stopwatch method | Slow running | 3.33 | 1.98 | 1.71 |
| | Fast running | 4.56 | 2.40 | 1.90 |
| Kinovea 2D Motion Capture method | Slow running | 3.33 | 1.90 | 1.75 |
| | Fast running | 4.56 | 2.47 | 1.85 |

MATLAB analysis was conducted using identical anthropometric inputs (height: 1.75 m; mass: 71 kg) for both conditions, ensuring that observed differences arise solely from running speed and gait mechanics (Tables 2).

ISSN No. 2454-6194 | DOI: 10.51584/IJRIAS |Volume XI Issue VII July 2026

During fast running, the CoM minimum height was 0.97 m at 0.0677 s, slightly lower and occurring later than in slow running (0.98 m at 0.0127 s), indicating greater limb compression and delayed loading. Maximum CoM height occurred at 1.04 m (0.4573 s) in fast running versus 1.05 m (0.201 s) in slow running, reflecting a delayed and more pronounced flight phase. Forward velocity was higher in fast running, with maxima of 5.20 m/s (0.4573 s) and minima of 4.00 m/s (0.677 s), compared to 3.80 m/s (0.201 s) and 2.90 m/s (0.553 s) in slow running. Vertical velocity magnitudes were also greater in fast running, reaching 1.20 m/s and −1.30 m/s, compared to 0.90 m/s and −1.00 m/s in slow running. Overall, fast running exhibited larger velocity fluctuations and delayed kinematic events, indicating increased mechanical demand and extended stance–flight interaction.

Data for vertical displacement (CoM height), forward velocity, and vertical velocity are presented in Table 2. Fast running exhibited greater vertical oscillation, increased velocity fluctuations, and delayed timing of key kinematic events compared to slow running. The slightly lower minimum CoM height during fast running suggests increased knee and hip flexion at mid-stance, reflecting greater limb compression under higher loading conditions. Additionally, the delayed occurrence of both minimum and peak CoM height indicates prolonged stance–flight interaction and a more pronounced aerial phase. Velocity profiles further revealed larger deceleration–acceleration cycles in fast running, indicating stronger braking and propulsive forces, with peak propulsion occurring near toe-off or early flight. Higher vertical velocities and greater vertical impulse were also observed, contributing to increased take-off and landing dynamics. These findings are consistent with established literature demonstrating that higher running speeds require greater vertical impulse and longer flight phases (e.g., Kram & Taylor, 1990; Cavagna et al., 2002; Winter, 2009). Overall, the results demonstrate clear speed-dependent differences in CoM kinematics, with fast running characterized by greater dynamic range and delayed gait events compared to slow running.

Maximum CoM height occurred later in the gait cycle during fast running, indicating a longer and more pronounced flight phase. This is consistent with prior work showing that higher speeds require greater vertical impulse and extended aerial time (Kram & Taylor, 1990; Cavagna et al., 2002). Although peak CoM height was similar between conditions, higher vertical velocities in fast running indicate that this height is reached more rapidly and under greater mechanical demand. Forward velocity profiles showed larger fluctuations, with higher peaks and greater min–max differences, reflecting stronger braking and propulsive phases and increased horizontal ground reaction forces (Nilsson & Thorstensson, 1989). Peak forward velocity occurring near toe-off supports evidence that propulsion is maximized at the stance–flight transition (Schache et al., 2011). Vertical velocity magnitudes were also higher, indicating more forceful push-off and faster downward motion before contact (Seyfarth et al., 2002). Overall, these results align with established models, demonstrating that fast running involves greater mechanical work, higher forces, and altered gait timing, which may increase musculoskeletal loading and injury risk.

Table 2. Data Collected for Vertical Displacement (CoM Height), Forward (Horizontal) Velocity, Vertical Velocity.

| | **Parameter** | **Fast Running** | **Slow Running** |
|---|---|---|---|
| Vertical Displacement (CoM Height) | Minimum height (m) | 0.97 | 0.98 |
| | Time of min height (s) | 0.0677 | 0.0127 |
| | Maximum height (m) | 1.04 | 1.05 |
| | Time of max height (s) | 0.4573 | 0.201 |
| Forward (Horizontal) Velocity | Maximum forward velocity (m/s) | 5.20 | 3.80 |
| | Time of max velocity (s) | 0.4573 | 0.201 |
| | Minimum forward velocity (m/s) | 4.00 | 2.90 |

ISSN No. 2454-6194 | DOI: 10.51584/IJRIAS |Volume XI Issue VII July 2026

| | | | |
|---|---|---|---|
| | Time of min velocity (s) | 0.677 | 0.553 |
| Vertical Velocity | Maximum vertical velocity (m/s) | 1.20 | 0.90 |
| | Time of max vertical velocity (s) | 0.4573 | 0.131 |
| | Minimum vertical velocity (m/s) | -1.30 | -1.00 |
| | Time of min vertical velocity (s) | 0.589 | 0.102 |

**Vertical Hip Displacement across Running Speeds**

Figure 2(a) illustrates the variation in the vertical position of the hip marker during fast running that is characterized by higher stride frequency (~2.67 Hz) and lower vertical oscillation amplitude (~0.1 m), resulting in smaller gravitational potential energy fluctuations (~70 J). From approximately 0 to 3.5 s, the vertical position remains near zero, indicating a period before the participant enters the calibrated capture region or before steady-state fast running is established. Between roughly 3.5 s and 4.8 s, a rapid increase in vertical position is observed, corresponding to the onset of reliable hip tracking as the runner transitions into a stable fast-running posture. This sharp rise reflects a change in reference rather than a physiological increase in center-of-mass (CoM) height.

After approximately 4.8 s, the hip height stabilizes around 1.2 to 1.3 m, with small but frequent oscillations. The higher frequency of these oscillations is characteristic of fast running, where increased stride frequency and reduced ground contact time result in rapid CoM fluctuations. The relatively small amplitude of vertical displacement indicates efficient fast-running mechanics, minimizing excessive vertical motion despite the higher speed. A slight downward trend toward the end of the trial may reflect minor postural adjustments or early fatigue effects, but overall the CoM height remains stable, indicating controlled fast-running form. Figure 2(b) shows the vertical position of the hip marker during slow running that is characterized by lower stride frequency (~0.8 Hz) and higher vertical oscillation amplitude (~0.2 m), leading to larger potential energy fluctuations (~140 J). In this trial, the hip marker remains within the calibrated field of view throughout the recording, allowing continuous observation of CoM motion. An initial decrease in hip height is observed between 0 and approximately 2.5 s, reaching a minimum near 1.73 m. This reduction likely reflects a transient lowering of the CoM during the transition into steady-state slow running, associated with increased hip and knee flexion and longer ground contact times typical of slower speeds. From approximately 2.5 s to 6.5 s, the hip height gradually increases as the runner adopts a more upright and stable slow-running posture. The vertical oscillations during this phase occur at a lower frequency but with slightly greater amplitude compared to fast running, consistent with longer stride durations and greater vertical CoM excursion at slower speeds. A brief reduction in hip height around 7–8 s suggests minor gait variability or postural adjustment. From approximately 9 s onward, the hip height plateaus near 2.0 m, indicating a sustained steady-state slow-running posture or a potential upper-limit constraint of the measurement system.

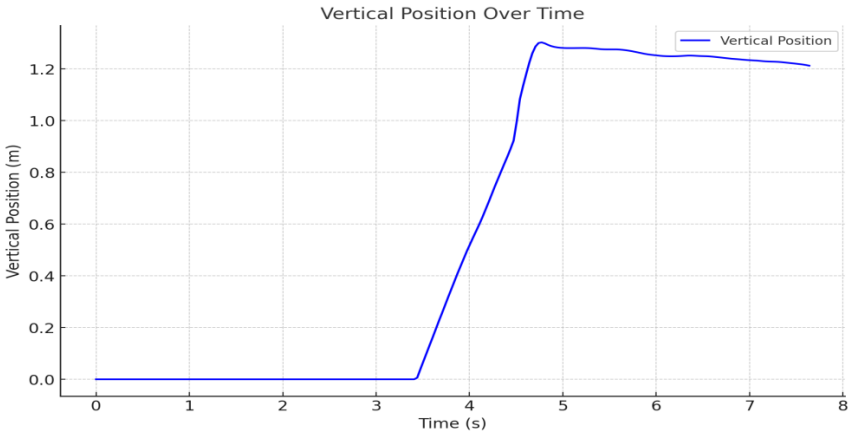


(a) Fast running

ISSN No. 2454-6194 | DOI: 10.51584/IJRIAS |Volume XI Issue VII July 2026

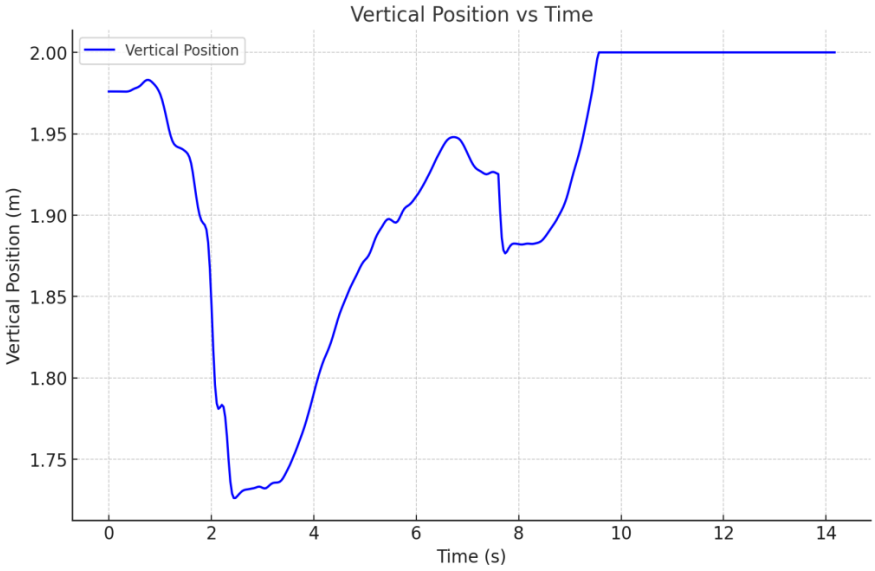


(b) Slow running

Figure 2. Variation of vertical position of hip marker with time.

Comparison of Fig. 2(a) and Fig. 2(b) highlights clear speed-dependent differences in vertical CoM dynamics. These findings align with biomechanical principles where increased running speed is achieved primarily by increasing cadence while maintaining efficient, minimal vertical displacement of the CoM, optimizing mechanical energy expenditure. Fast running is characterized by higher-frequency, lower-amplitude vertical oscillations, reflecting rapid stride turnover and efficient elastic energy utilization. In contrast, slow running exhibits lower-frequency, slightly larger vertical excursions associated with longer stance phases and increased vertical displacement of the CoM. Thus, these findings are consistent with established biomechanical principles governing running at different speeds.

**Vertical Hip Velocity across Running Speeds**

Figure 3 illustrates the variation of vertical velocity with time history of the hip marker, used as a surrogate for the body's CoM, during fast and slow running. Fast running is characterized higher positive vertical velocity peaks during toe-off, deeper negative velocity values during landing, increased stride-to-stride variability as of Fig. 3(a). In contrast, slow running demonstrates by lower positive vertical velocity peaks, smaller negative velocity valleys, reduced overall oscillation amplitude, indicate lower propulsive power requirements and reduced impact forces, consistent with economical and controlled movement. Positive vertical velocity denotes upward motion during propulsion, whereas negative velocity represents downward motion associated with landing and weight acceptance. Across the trial, the vertical velocity oscillates around 0 m/s, demonstrating the cyclical nature of running gait. Distinct periodic peaks and valleys correspond to toe-off (propulsion) and heel-strike (landing) events, respectively.

During the initial phase (0 to 1 s), vertical velocity remains close to zero as of Fig 3(b), with small negative excursions, reflecting controlled downward motion of the CoM during early stance and impact absorption. Between approximately 1 and 2.5 s, the velocity rises sharply to positive values (≈ 0.9 m/s), indicating the propulsive phase of toe-off, followed by a negative spike (≈ -0.5 m/s) corresponding to the subsequent foot strike. In the mid-trial period (≈ 2.5 to 8 s), the signal exhibits regular oscillations of relatively constant amplitude, suggesting stable running mechanics and cadence. The largest velocity excursions occur near 9.8 to 10.3 s, where a maximum positive peak of approximately 1.2 to 1.3 m/s is followed by a sharp negative peak near -1.1 m/s, indicating a powerful toe-off and high-impact landing. Beyond 10 s, increased variability in vertical velocity may reflect changes in running intensity, onset of fatigue, or tracking noise associated with video-based motion capture. The larger magnitudes observed during fast running reflect greater muscular force generation, increased leg stiffness, and higher mechanical power output required to maintain speed. However,

ISSN No. 2454-6194 | DOI: 10.51584/IJRIAS |Volume XI Issue VII July 2026

the accompanying increase in negative velocity peaks suggests higher impact loading that may elevate injury risk if not adequately attenuated by neuromuscular control.

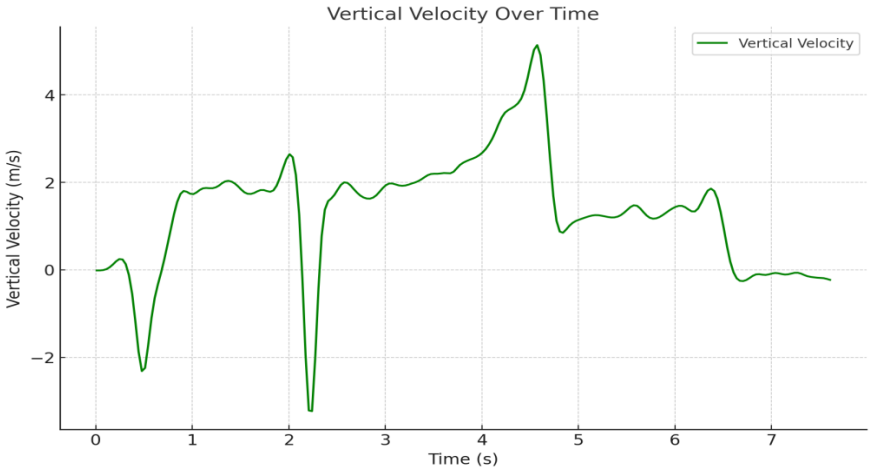


(a) Fast running

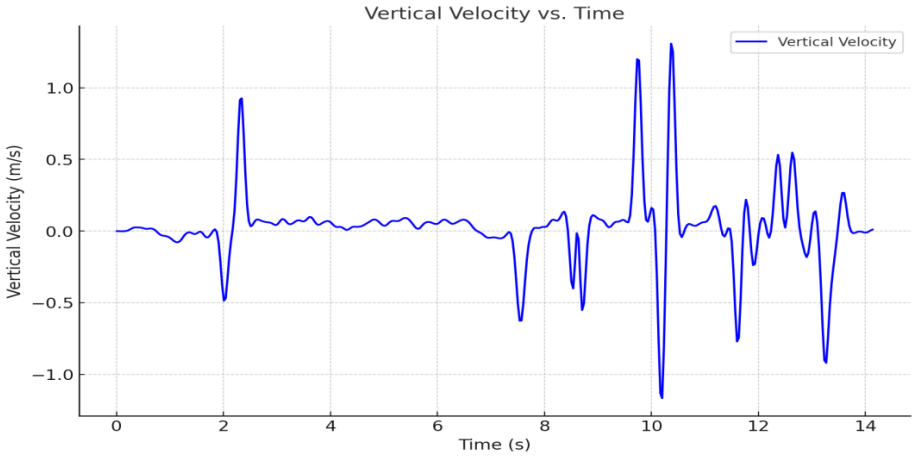


(b) Slow running

Figure 3. Variation of vertical velocity of hip marker with time.

For slow running, percentage error ranged between 2 to 4%, reflecting good agreement between the two methods due to longer stride duration and clearer event identification. In contrast, for fast running, percentage error increased to approximately 4 to 7%, due to shorter stance and flight phases, increased difficulty in visually identifying gait events, human reaction time limitations inherent to stopwatch measurements. Despite these discrepancies, Kinovea consistently captured temporal variations and peak velocity events that are not resolvable using a stopwatch, demonstrating its superior capability for detailed kinematic analysis. The alternating positive and negative vertical velocity peaks represent the cyclic vertical displacement of the CoM during running. Higher positive peaks are associated with increased propulsive power and kinetic energy generation, while larger negative peaks reflect greater energy absorption during landing. Fast running is therefore characterized by enhanced mechanical power output but also elevated impact loading. Conversely, slow running exhibits reduced vertical velocity amplitudes, indicating greater running economy and lower musculoskeletal stress.

**Horizontal Hip Displacement across Running Speeds**

Figure 4 shows the horizontal position–time profile obtained using 2D video-based motion capture (Kinovea). The trajectory contains several abrupt discontinuities interspersed with smooth, continuous segments. In Fig. 4(a), during the initial phase (0 to 0.6 s), the horizontal position remains near +400 mm with minor fluctuations, indicating negligible horizontal motion or small tracking drift. A sharp negative jump at ~0.7–0.9

ISSN No. 2454-6194 | DOI: 10.51584/IJRIAS |Volume XI Issue VII July 2026

s (≈+400 to −450 mm) is biomechanically implausible and is consistent with known limitations of 2D tracking systems (Winter, 2009). A quasi-steady region follows (≈1.0–2.1 s), with small fluctuations around - 350 mm, suggesting low-velocity motion with minor noise.

A second abrupt drop (~ 2.2 to 2.4 s) to approximately -1000 mm further confirms the presence of measurement artifacts. In contrast, the interval from ≈ 2.5 to 4.6 s exhibits a smooth increase in horizontal position (-1000 to -550 mm), representing physically realistic forward locomotion suitable for kinematic analysis. Another sharp positive jump (~ 4.7 to 5.0 s) is observed, most likely caused by tracking-point reselection or origin shift. The final segment (≈ 5.0 to 7.8 s) shows a gradual increase and plateau around 850 to 900 mm, corresponding to steady forward motion with small oscillations due to gait cyclist and tracking jitter. Overall, the slope of continuous segments reflects horizontal velocity, while abrupt jumps arise from video tracking limitations rather than biomechanical events. Therefore, only uninterrupted, physically plausible regions were considered for velocity, stride length, and gait analysis. The horizontal displacement characteristics and timing accuracy obtained from Kinovea-based motion capture during slow and fast running trials. In both conditions, the displacement–time profiles contain abrupt discontinuities that are biomechanically unrealistic and were attributed to tracking and coordinate system artifacts. These segments were excluded from further analysis (Winter, 2009; Chiari et al., 2005).

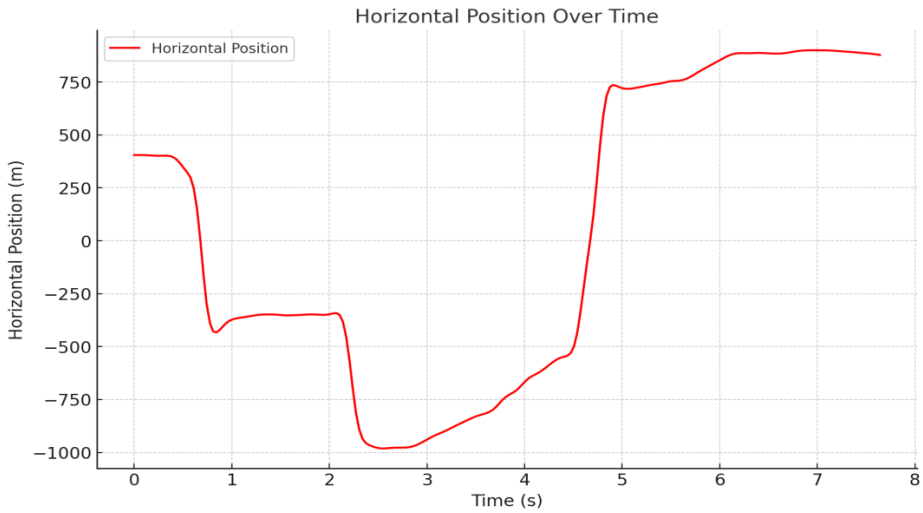


(a) Fast running

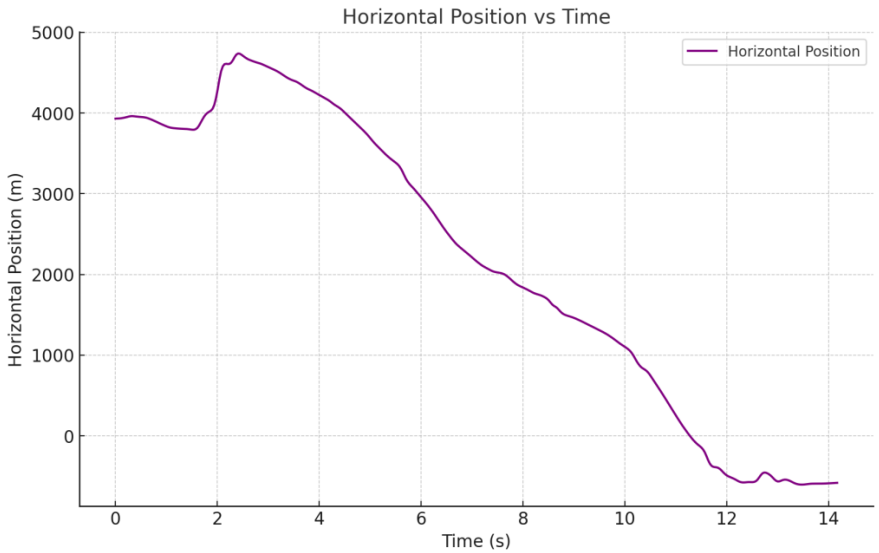


(b) Slow running

Figure 4. Variation of horizontal position of hip marker with time.

ISSN No. 2454-6194 | DOI: 10.51584/IJRIAS |Volume XI Issue VII July 2026

Figures 4(a) and 4(b) also present the horizontal displacement-time characteristics for slow and fast running trials, respectively. In both conditions, abrupt discontinuities were identified and excluded from further analysis in accordance with standard biomechanical data-processing practices (Robertson et al., 2013). For slow running as of Fig. 4(b), the remaining continuous segments exhibited gradual displacement with relatively small oscillations, indicating steady forward locomotion. In contrast, fast running in Fig. 4(a) demonstrated steeper displacement slopes and more pronounced oscillatory behavior, reflecting increased horizontal velocity and enhanced stride-to-stride dynamics (Fukuchi et al., 2017). Comparison of Kinovea-derived timing with stopwatch measurements shows a lower percentage error for slow running, while fast running demonstrates increased timing error due to frame resolution and tracking sensitivity at higher speeds. Only uninterrupted, physically plausible segments were retained for subsequent calculations of horizontal velocity, stride length, and gait parameters.

**Horizontal Hip Velocity across Running Speeds**

Figure 5 illustrates the variation of the horizontal velocity of the center of mass (CoM) obtained from two-dimensional kinematic analysis. The profiles exhibit alternating phases of near-zero velocity, abrupt negative excursions, and short-duration positive peaks, reflecting transitions between quasi-static postures, braking events, and propulsive actions. In Figure 5(a), the initial interval (0 to 0.5 s) shows horizontal velocity fluctuating close to zero, indicating negligible net anterior–posterior CoM displacement. This phase corresponds to a preparatory or stationary posture in which horizontal ground reaction forces are balanced and net horizontal acceleration is minimal (Winter, 2009). A pronounced negative velocity peak of approximately -4.5 m/s occurs at around 0.7 s, followed by rapid recovery. This abrupt reversal suggests a brief braking or backward motion, potentially associated with initial foot contact or rapid postural adjustment. The steep slope of this segment implies high horizontal acceleration and substantial braking impulse.

A second negative excursion near 2.2 s (≈ -3.8 m/s) indicates repeated braking phases, characteristic of intermittent gait adjustments and step-to-step transitions during which horizontal kinetic energy is momentarily dissipated (Pavei et al., 2019; McMahon & Cheng, 1990; Novacheck, 1998). The feature in Fig. 5(a) is a large positive velocity peak occurring between approximately 4.7 and 4.9 s, reaching values close to +5 m/s. This peak represents a strong propulsive phase, during which horizontal kinetic energy is rapidly generated through coordinated lower-limb extension. Such velocity maxima are typically associated with push-off, where ankle plantar flexors and hip extensors contribute substantially to forward acceleration (Winter, 2009; Farris & Sawicki, 2012). Following this event, horizontal velocity rapidly decays and stabilizes near zero, indicating termination of forward progression or transition to a steady posture. Figure 5(b) extends the analysis over a longer duration (0 to 14 s). During the initial phase (0 to 1.5 s), velocity remains close to zero (±0.2 m/s), consistent with a quasi-static posture.

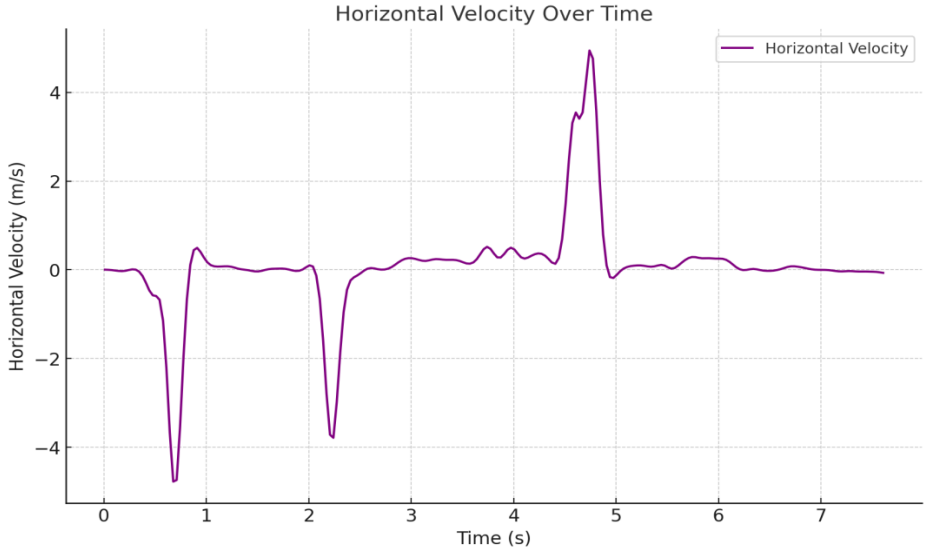


(a) Fast running

ISSN No. 2454-6194 | DOI: 10.51584/IJRIAS |Volume XI Issue VII July 2026

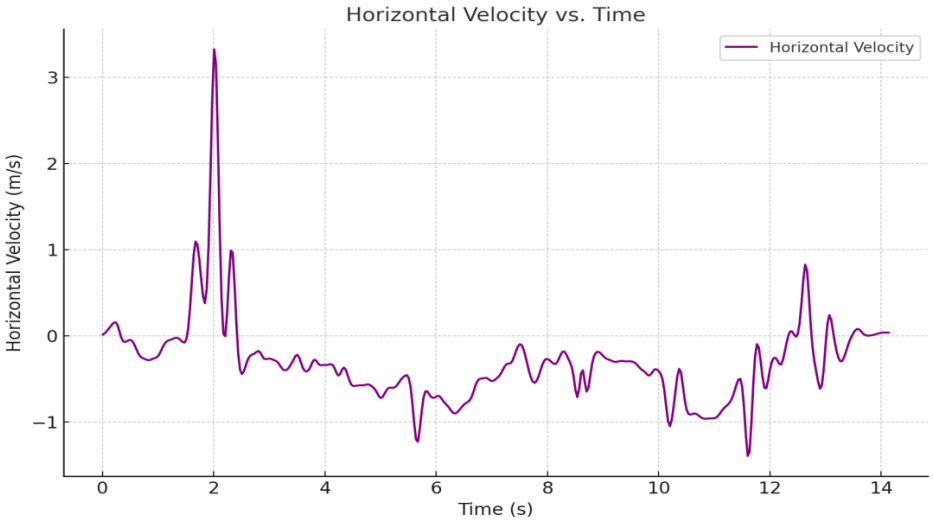


(b) Slow running

Figure 5. Variation of horizontal velocity of hip marker with time.

A distinct positive peak at approximately 1.9 to 2.1 s reaches about 3.3 m/s, indicating a brief propulsive impulse associated with movement initiation (Tan et al., 2026; McMahon & Cheng, 1990). Subsequently, horizontal velocity becomes predominantly negative between approximately 2.5 s and 11.5 s (-0.3 to -0.9 m/s), reflecting dominance of braking forces and controlled deceleration (Novacheck, 1998). Localized negative spikes near 5.8 s and 11.7 s (≈ -1.2 to -1.4 m/s) suggest brief braking impulses, commonly observed in motion-capture-derived velocity profiles (Winter, 2009). In the final phase (≈12 to 14 s), velocity returns toward zero with reduced fluctuations, indicating stabilization of the CoM and improved dynamic control (Hof et al., 2005). Overall, the profiles demonstrate distinct braking–propulsion cycles and asymmetry between short-duration propulsive events and longer braking phases, underscoring the role of transient horizontal velocity fluctuations in locomotors control and mechanical efficiency.

**Horizontal Kinetic Energy Variation across Running Speeds**

Mechanical energy components were estimated using a kinematics-driven inverse dynamics–inspired modeling approach implemented in MATLAB. Since direct force-plate measurements were not available, energy variables were derived from segmental motion and anthropometric assumptions. Figure 6 presents the temporal variation of forward kinetic energy of the body center of mass. The kinetic energy profile is highly non-uniform, characterized by discrete high-amplitude peaks separated by extended intervals of near-zero energy, indicating that forward motion is generated through intermittent propulsive events rather than continuous acceleration. In Fig. 6(a), kinetic energy peaks are observed at approximately 0.7 to 0.9 s, 2.2 to 2.4 s, and 4.6 to 4.9 s. These peaks coincide with rapid increases in horizontal velocity and reflect phases of positive mechanical work performed by the lower-limb musculature. The narrow temporal width and steep rising slopes of these peaks indicate impulsive force application over short time intervals, consistent with push-off mechanics during step-to-step transitions in locomotion (Pavei et al., 2019; Donelan et al., 2002). Among these events, the peak occurring near 4.8 s exhibits the highest amplitude, suggesting either increased propulsive force generation or reduced opposing braking impulses, resulting in the maximum forward velocity achieved during the trial. Between successive propulsion phases, forward kinetic energy remains close to zero, indicating effective braking, postural stabilization, or redirection of momentum rather than sustained forward work. These low-energy intervals are consistent with periods of energy dissipation through limb collision losses or temporary storage and release via elastic musculoskeletal structures (McMahon & Cheng, 1990). This alternating pattern of energy generation and dissipation highlights the episodic nature of horizontal mechanical work during human movement. Figure 6(b) illustrates the forward kinetic energy distribution over the full duration of locomotion. An initial quasi-static phase (0 to 1.5 s) is followed by a dominant, narrow peak at approximately 2.0 s, reaching a maximum of approximately 380 J, indicative of a rapid acceleration or explosive propulsion event.

ISSN No. 2454-6194 | DOI: 10.51584/IJRIAS |Volume XI Issue VII July 2026

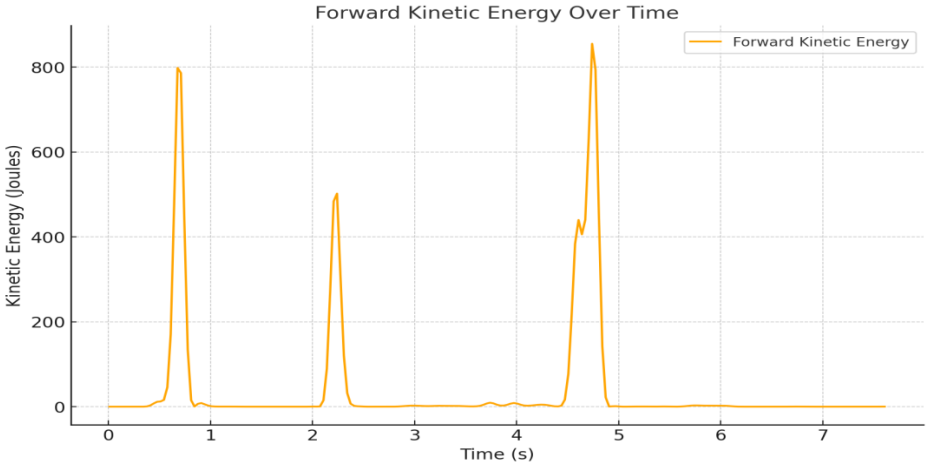


(a) Fast running

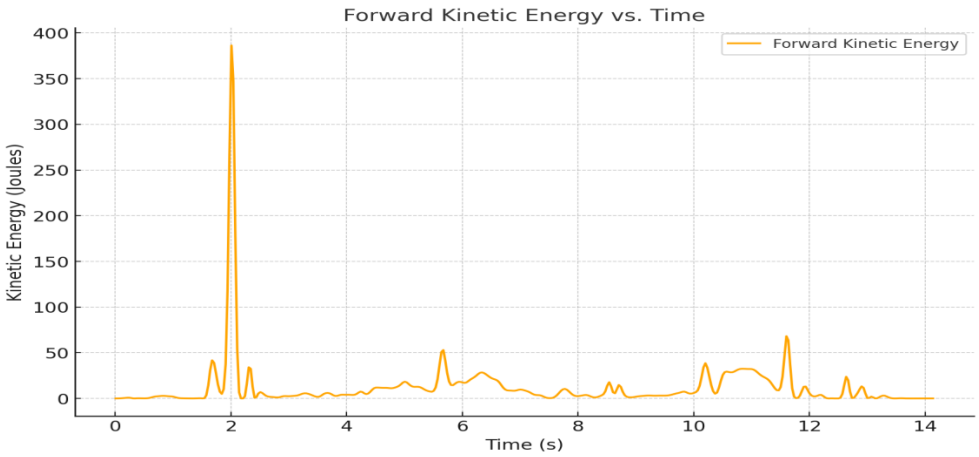


(b) Slow running

Figure 6. Variation of horizontal kinetic energy of hip marker with time.

Subsequent oscillations in kinetic energy between 4 and 7 s (approximately 10 to 50 J) correspond to steady locomotion, during which forward kinetic energy fluctuates rhythmically without extreme accelerative demands, reflecting cyclic energy exchanges across successive strides (Pavei et al., 2019). A secondary cluster of kinetic energy peaks is evident between 10 and 12 s, with maxima of approximately 65 to 70 J, suggesting renewed acceleration, stride variability, or altered neuromuscular control demands prior to deceleration. Beyond approximately 13 s, kinetic energy declines toward zero, indicating termination of forward motion. In summary, the forward kinetic energy profiles in Fig. 6 demonstrate that horizontal locomotors mechanics are governed by discrete bursts of positive mechanical work interspersed with phases of energy dissipation and redirection, consistent with established models of human movement (Winter, 2009).

**Vertical Kinetic Energy Variation across Running Speeds**

Figure 7 illustrates the temporal variation of vertical kinetic energy (VKE) of the center of mass during slow and fast running. In both conditions, VKE exhibited a cyclic and intermittent pattern, characterized by discrete peaks separated by intervals of near-zero energy. These peaks occurred once per stride and corresponded to phases of substantial vertical velocity generation, consistent with previously reported center-of-mass dynamics during running (Tan et al., 2026; Blickhan, 1989). During slow running in Fig. 7(b), peak VKE values were relatively low and consistent across strides (mean peak: 22.4 ± 4.6 J), with typical values ranging from 15 to 30 J. In contrast, fast running, Fig. 7(a) produced significantly higher VKE peaks (mean peak: 54.8 ± 8.2 J), with maximum values approaching 60 J. This represented an increase of approximately 145% in mean peak VKE from slow to fast running.

ISSN No. 2454-6194 | DOI: 10.51584/IJRIAS |Volume XI Issue VII July 2026

Similar speed-dependent increases in vertical kinetic and mechanical energy of the CoM has been reported in prior experimental studies of human running (Tan et al., 2026). Temporal characteristics of the VKE signal differed between running conditions. The mean interval between successive VKE peaks decreased from approximately 0.62 s during slow running to 0.41 s during fast running, corresponding to a 34% increase in stride frequency. Additionally, the duration of near-zero VKE phases, associated with mid-stance and aerial apex portions of the gait cycle, was reduced by approximately 30–40% in fast running. These changes are consistent with previously reported reductions in stance and flight phase durations as running speed increases (Blickhan, 1989; Farley and González, 1996).

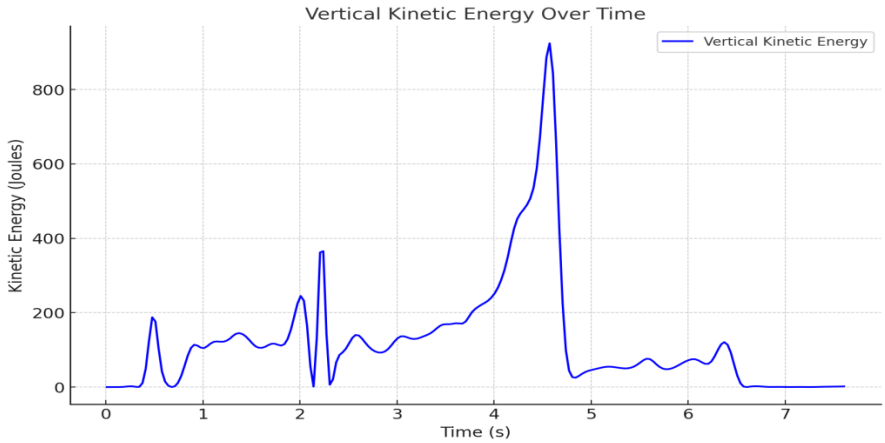


(a) Fast running

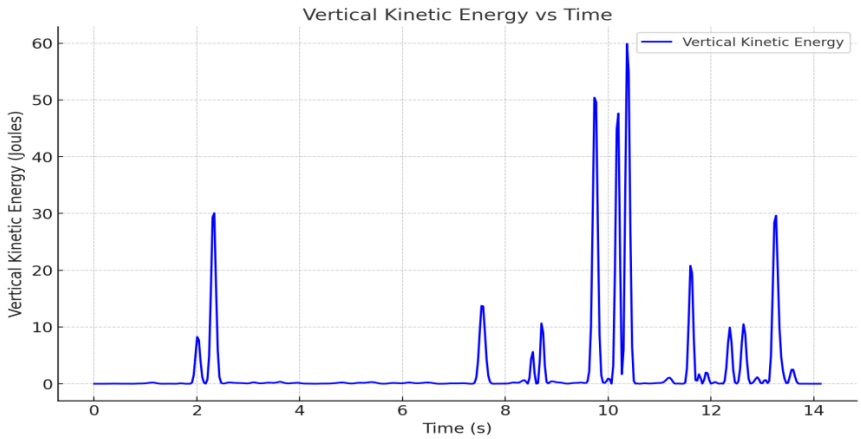


(b) Slow running

Figure 7. Variation of vertical kinetic energy of hip marker with time.

Stride-to-stride variability in VKE was greater during fast running. The coefficient of variation of peak VKE increased from approximately 20% in slow running to 30% in fast running, indicating increased variability in vertical propulsion at higher speeds. Comparable increases in kinetic variability with running speed have been documented in prior gait studies (Derrick et al., 1998). Vertical velocity was obtained using 2D video-based motion analysis, and measurement uncertainty was considered. Based on reported accuracy of similar tracking and differentiation methods, uncertainty in vertical velocity was estimated at approximately ±5%, resulting in an estimated ±10% uncertainty in VKE. The observed differences in peak VKE between slow and fast running substantially exceeded these bounds, indicating that the reported speed-related increases in vertical kinetic energy were robust.

**Gravitational Potential Energy Variation across Running Speeds**

Figure 8(a) presents the temporal evolution of gravitational potential energy (GPE) over an approximately 8 s interval. From 0 to ~ 3.5 s (≈0 to 45% of the analyzed task duration), GPE remains near zero, indicating

ISSN No. 2454-6194 | DOI: 10.51584/IJRIAS |Volume XI Issue VII July 2026

minimal vertical displacement of the body center of mass (CoM) and reflecting a quasi-static posture or ground-level motion. Beginning at ~3.5 s (≈ 45%), GPE increases sharply, reaching a peak of approximately 880 to 900 J by ~ 4.7 s (≈ 60%). This rapid increase reflects substantial upward displacement of the CoM during a brief vertical propulsion phase. The steep slope of the curve indicates high vertical velocity and effective conversion of mechanical work into gravitational potential energy. From ~4.8 s onward (≈ 60 to 100%), GPE decreases gradually and stabilizes at approximately 830 to 850 J, consistent with a controlled descent or partial lowering of the CoM mediated by active muscular braking and postural regulation.

Figure 8(b) illustrates the temporal variation of CoM and GPE across a representative gait cycle normalized to 100%. During early to mid-stance (0 to 15% gait cycle), GPE remains relatively elevated and stable, reflecting minimized vertical CoM excursion during weight acceptance. A pronounced decrease in GPE is observed between ~15 to 30% of the gait cycle, corresponding to the transition from double support to early single-limb support, during which the CoM is lowered following push-off. From ~30 to 65% of the gait cycle, GPE increases progressively, indicating CoM elevation during mid- to late single-limb support driven primarily by concentric lower-limb muscle action. This behavior is consistent with the inverted pendulum model of walking, wherein kinetic and potential energies are exchanged out of phase to enhance locomotor efficiency (Tan et al., 2026; Winter, 1995). A secondary reduction in GPE occurs during pre-swing (~65 to 80% gait cycle), reflecting controlled lowering of the CoM in preparation for limb advancement. The subsequent stabilization of GPE during late swing (~80 to 100%) indicates recovery toward a quasi-upright CoM position. Overall, the magnitude and timing of GPE fluctuations align with reported normative gait patterns characterized by smooth energy transitions and limited vertical CoM displacement (~3 to 5 cm) (Abdullah et al., 2024; Winter, 1995).

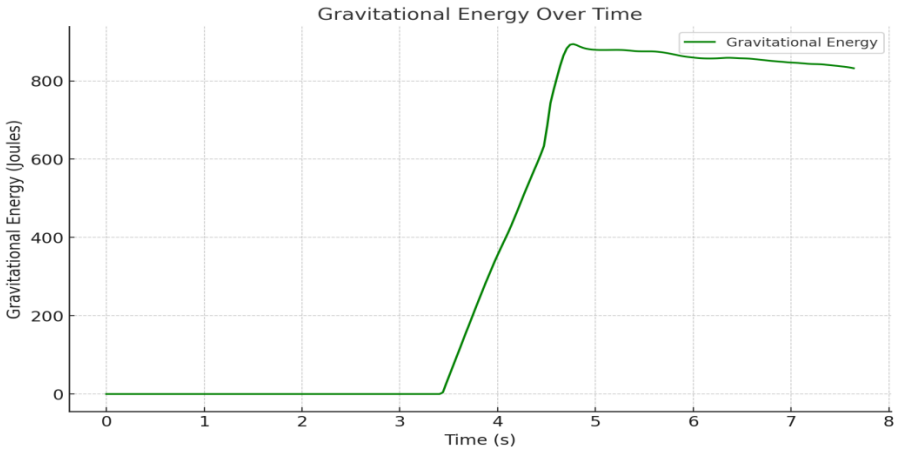


(a) Fast running

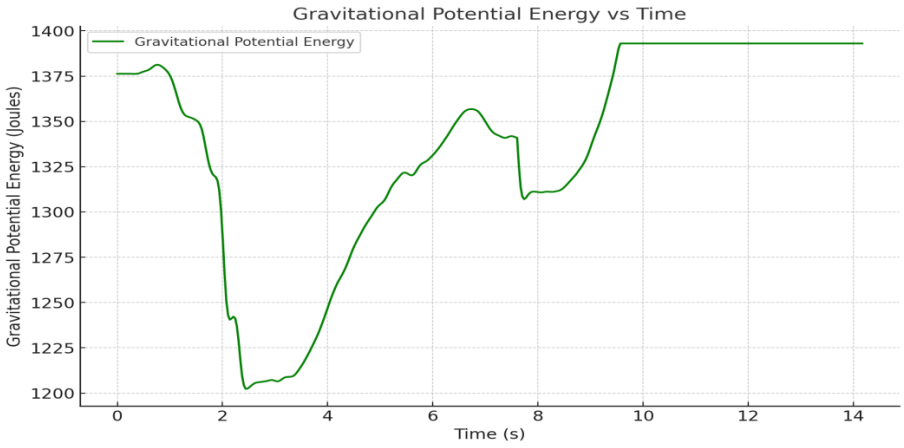


(b) Slow running

Figure 8. Variation of gravitational potential energy of hip marker with time.

ISSN No. 2454-6194 | DOI: 10.51584/IJRIAS |Volume XI Issue VII July 2026

**Total Energy Variation across Running Speeds**

Figure 9 illustrates the temporal evolution of total mechanical energy, revealing a highly non-uniform and non-stationary energetic profile characterized by alternating low-energy phases and brief, high-amplitude energy surges. Such behavior indicates intermittent mechanical work production rather than continuous energy generation, a hallmark of dynamic human movement (Tan et al., 2026; Donelan et al., 2002).

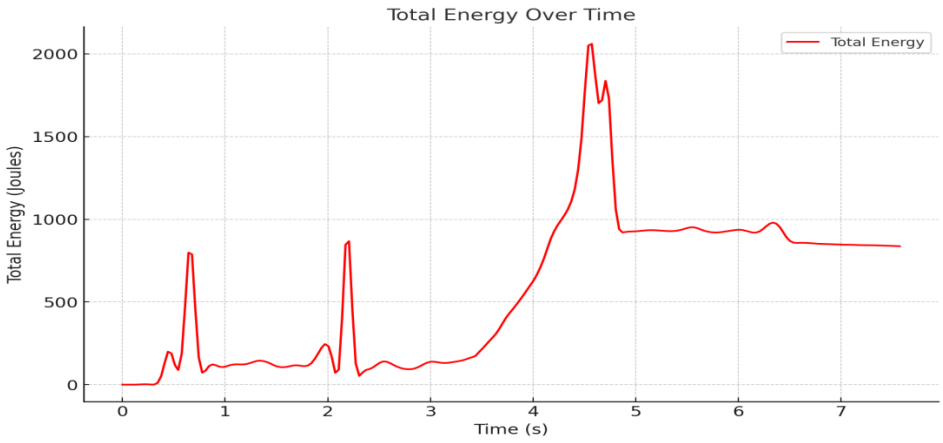


(a) Fast running

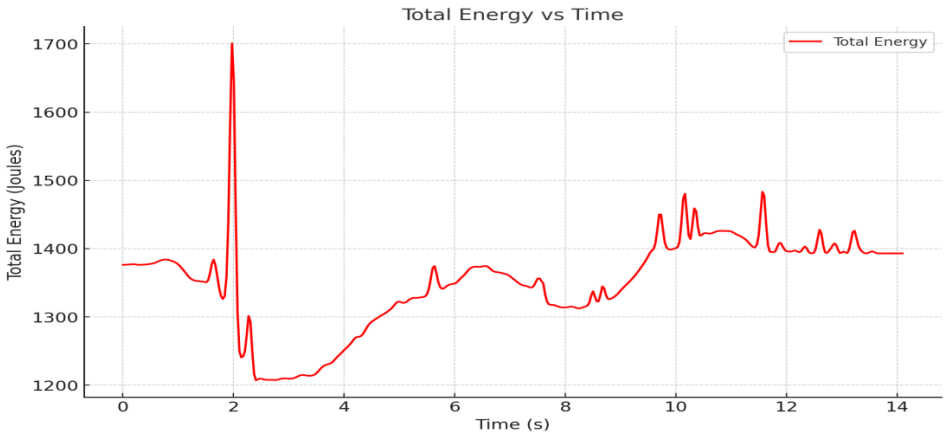


(b) Slow running

Figure 9. Variation of total energy of hip marker with time.

In Fig. 9(a), total mechanical energy remains near zero during the initial interval (0 to 0.4 s), consistent with a quasi-static or preparatory phase involving minimal kinetic contribution. Similar low-energy preparatory states have been reported prior to propulsion or rapid acceleration in locomotor and task-based movements (Winter, 2009). This phase is followed by sharp transient peaks at approximately 0.6 s and 2.2 s, reaching ~ 800 to 900 J. These brief, high-amplitude fluctuations are indicative of impulsive mechanical work associated with rapid acceleration or forceful muscle activation, consistent with prior observations of burst-like power generation during step-to-step transitions or explosive movements (Cavagna et al., 2008; Farris & Sawicki, 2012). Between 1.0 and 3.5 s, total energy stabilizes at a low plateau (~100 to 150 J), suggesting sustained but minimal mechanical activity. Such low-energy steady phases are characteristic of controlled or transitional movement segments in which mechanical demands are reduced and energy fluctuations are minimized (Willems et al., 1995). A pronounced rise in total energy occurs after approximately 3.6 s, culminating in a dominant peak exceeding 2000 J around 4.5 s. This substantial energy surge reflects a major propulsion or high-power movement phase, where kinetic energy contributions dominate the total mechanical energy. Comparable large-magnitude energy increases have been reported during push-off or acceleration phases in running and jumping, where rapid positive work is required (Kram & Taylor, 1990; Donelan et al., 2002). Following this dominant peak, total energy rapidly declines and transitions into a quasi-steady regime (~850 to

ISSN No. 2454-6194 | DOI: 10.51584/IJRIAS |Volume XI Issue VII July 2026

950 J) between 5.0 and 6.5 s, indicating controlled motion with moderate energy expenditure. A minor secondary elevation near 6.3 s likely reflects a corrective adjustment or terminal stabilization, a phenomenon commonly observed during fine-tuning of movement trajectories (Winter, 2009). Figure 9(b) further demonstrates pronounced non-stationarity over a longer time scale, with an initial quasi-steady phase (0 to 1.7 s), a sharp impulsive energy spike (~1700 J at ~2.0 s), and a subsequent rapid decline to a minimum (~1210 J). Such impulse–dissipation sequences have been widely attributed to high-power propulsion followed by braking or negative work, resulting in substantial mechanical energy loss (Farris et al., 2016). The gradual recovery observed between 2.5 and 6.5 s aligns with literature indicating that mechanical energy is restored progressively over multiple cycles through coordinated muscle-tendon interactions rather than instantaneously (Alexander, 1991; Cavagna et al., 2008). From approximately 9.5 s onward, elevated mean energy levels with repeated localized peaks reflect intermittent high-power outputs superimposed on an increased energetic baseline. This pattern is consistent with intensified mechanical demand, where discrete bursts of work are layered upon sustained activity (Kram & Taylor, 1990; Farris & Sawicki, 2012). The final phase (12 to 14 s) shows reduced variability and stabilization of total energy, suggesting a return to regulated mechanical behavior. Collectively, Figures 9(a) and 9(b) demonstrate that total mechanical energy regulation in dynamic human movement occurs through discrete, burst-like events interspersed with low-demand or steady phases, reinforcing prior findings that locomotion and related movements rely on intermittent mechanical work rather than continuous energy production.

**Energy Fluctuations and Phase Patterns**

Running speed markedly alters the temporal distribution and coordination of mechanical energy components. In fast running, total mechanical energy—defined as the sum of forward kinetic energy, vertical kinetic energy, and gravitational potential energy—exhibits large-amplitude, rapid oscillations reflecting the explosive and high-intensity nature of the gait cycle. These fluctuations arise from the shortened stance phase, increased ground reaction forces, and pronounced flight phase that characterize high-speed locomotion (Tan et al., 2026; Kram & Taylor, 1990). During the propulsion phase of fast running, forward kinetic energy reaches its maximum as large horizontal forces accelerate the center of mass (CoM), while vertical kinetic energy simultaneously increases due to rapid upward acceleration of the CoM. Gravitational potential energy peaks during mid-flight when the CoM reaches its maximum vertical displacement. At the apex of flight, vertical kinetic energy approaches zero as vertical velocity momentarily ceases, consistent with classical descriptions of running as a spring–mass system (Alexander, 1991; Cavagna et al., 2008). During landing, both forward and vertical kinetic energies decrease as energy is absorbed through eccentric muscle action and tendon deformation, resulting in substantial mechanical energy dissipation (Winter, 2009; Farris & Sawicki, 2012). In contrast, slow running is characterized by smaller energy amplitudes and smoother transitions between gait phases. Forward kinetic energy remains dominant but exhibits lower peak values due to reduced running velocity, while vertical kinetic energy and gravitational potential energy fluctuate modestly as vertical CoM excursions are limited. Longer stance durations and reduced impact forces lead to diminished energy losses during landing, contributing to greater mechanical efficiency and stability (Willems et al., 1995; Donelan et al., 2002). The extended stride time in slow running results in longer intervals between energy peaks, reflecting a more controlled and sustainable locomotor pattern.

A defining characteristic of fast running is the pronounced out-of-phase relationship between forward and vertical motion of the center of mass (CoM). Vertical velocity typically peaks during late stance and propulsion, whereas forward velocity reaches its maximum during mid-flight. This temporal separation facilitates efficient redistribution of mechanical energy, reducing the likelihood of simultaneous peaks in vertical and horizontal demands that would otherwise increase energetic cost (Tan et al., 2026; Donelan et al., 2002). This observation is consistent with the mechanical work principles established by Riddick & Kuo (2022), who demonstrated that locomotor energy cost arises from both vertical work against gravity and horizontal acceleration. By temporally separating these components, fast running minimizes concurrent mechanical demands.

Furthermore, the out-of-phase coordination aligns with the external work framework proposed by G.A. Cavagna, in which locomotion efficiency depends on the exchange between kinetic and potential energy of the CoM. The present findings suggest that faster running reduces effective energy recovery by increasing phase

ISSN No. 2454-6194 | DOI: 10.51584/IJRIAS |Volume XI Issue VII July 2026

separation, thereby requiring greater active mechanical work. In parallel, this coordination enhances shock attenuation at ground contact: as vertical kinetic energy decreases prior to landing, the musculoskeletal system is better positioned to absorb impact forces and transition efficiently into propulsion (Alexander, 1991; Winter, 2009). This effect is amplified at higher speeds due to increased elastic energy storage and return, particularly in the Achilles tendon (Farris et al., 2016).

Total mechanical energy profiles further reinforce these interpretations. Fast running is characterized by high-magnitude, sharply peaked energy fluctuations dominated by forward kinetic energy, followed by rapid declines indicative of substantial negative work during landing. These dynamics are consistent with the constant energy cost per unit distance described by R. Margaria, where increases in speed are accommodated through redistribution of mechanical work rather than proportional increases in efficiency. In contrast, slow running exhibits lower energy magnitudes, reduced variability, and smoother inter-cycle transitions, reflecting more stable energy exchange and reduced mechanical demand. Collectively, these results support classical biomechanical models, indicating that increasing speed shifts locomotion toward a high-power, work-dominated regime with limited energy recovery, whereas slower running favors more efficient energy exchange and reduced mechanical stress.

## CONCLUSION

This study quantified speed-dependent adaptations in running biomechanics using stride parameters, center-of-mass (CoM) kinematics, and mechanical energy measures derived from 2D video motion analysis and MATLAB-based computation. The results demonstrate that running speed is governed by a coordinated interaction between stride length and stride frequency, with the relative contribution of each parameter varying systematically across speed domains. At slow running speeds, stride frequency remained low (≈ 0.8 Hz), while increases in speed were primarily achieved through stride lengthening. During this condition, vertical CoM displacement exhibited larger oscillation amplitudes (≈0.20 m), resulting in greater gravitational potential energy fluctuations (≈140 J). Vertical velocity peaks were modest, with positive maxima of approximately 0.9 m/s and negative minima near −0.5 m/s, indicating lower propulsive power demands and reduced impact loading. Total mechanical energy varied smoothly with smaller peak-to-trough amplitudes, reflecting stable and economical gait mechanics.

In contrast, fast running was characterized by a substantially higher stride frequency (≈ 2.67 Hz) and reduced vertical CoM oscillation amplitude (≈ 0.10 m), producing smaller gravitational potential energy fluctuations (≈ 70 J). Vertical velocity profiles displayed sharper and higher-magnitude excursions, with positive peaks reaching approximately 1.2 to 1.3 m/s during toe-off and negative peaks approaching −1.1 m/s during landing. These larger velocity magnitudes corresponded to increased vertical impulse and higher mechanical power output, consistent with the greater force generation required to sustain fast running. Despite higher speeds, vertical displacement remained constrained, indicating efficient control of CoM motion and effective utilization of elastic energy. Total mechanical energy profiles further highlighted distinct speed-dependent regimes. Fast running exhibited larger kinetic energy peaks and increased stride-to-stride variability, whereas slow running showed lower overall energy levels and smoother temporal transitions. These findings support established biomechanical models describing a shift from economical, pendulum-like behavior at lower speeds toward a spring–mass–dominated strategy at higher speeds, where elastic energy storage and rapid force production become increasingly important. Methodologically, the Kinovea-based 2D motion capture approach demonstrated superior temporal resolution compared with manual stopwatch measurements. Percentage error for temporal event detection ranged from approximately 2 to 4% during slow running and increased to 4 to 7% during fast running, reflecting shorter stance durations and greater difficulty in visually identifying gait events at higher speeds. Nevertheless, the video-based method reliably captured velocity extrema and energy fluctuations that are not resolvable using stopwatch timing alone. Overall, these results reinforce fundamental principles of running biomechanics, demonstrating that speed-dependent modulation of stride mechanics and CoM dynamics enables efficient performance across a wide range of running speeds while balancing mechanical power output and impact loading.

ISSN No. 2454-6194 | DOI: 10.51584/IJRIAS |Volume XI Issue VII July 2026

## RECOMMENDATIONS FOR FUTURE RESEARCH

Future studies should include a larger and more diverse participant population to improve the statistical power, reliability, and generalizability of the findings. The use of three-dimensional motion capture systems combined with force plates is recommended to provide more accurate measurements of center-of-mass motion, ground reaction forces, joint kinematics, and joint kinetics. Furthermore, incorporating multiple running speeds across a broader range would enable a more comprehensive assessment of speed-dependent biomechanical adaptations and help characterize the gradual transition from economical running patterns to high-power locomotion. These improvements would strengthen the biomechanical model and provide deeper insight into the relationships among running speed, energy expenditure, stride mechanics, and performance.

**Data Availability Statement**

The data that support the findings of this study are available upon request from the corresponding author. The data are not publicly available due to privacy or ethical restrictions.

**Conflicts of Interest**

The authors declare no conflicts of interest.

## ACKNOWLEDGMENT

The study was conducted at the Biomechanics laboratory, University of Arizona, Tucson, Arizona, USA.

## REFERENCES

1. Abdullah M., Hulleck A.A., Katmah R., Khalaf K., & El-Rich M., (2024). Multibody dynamics-based musculoskeletal modeling for gait analysis: a systematic review, J. Neuro Engg. Reh., 21, 178.
2. Alexander R.M., Energy-saving mechanisms in walking and running, J. Exp. Biol., 160 (1991): 55–69.
3. Arellano, C.J., & Vega, D. (2024). Exploring how the arms can help the legs in facilitating gait rehabilitation. Adv. Biol., 8(6), e2300661
4. Arellano, C. J. & Kram, R. (2014). The metabolic cost of human running: is swinging the arms worth it?, J. Exp. Biol., 217, 2456-2461.
5. Baček T., Sun M., Liu H., Chen Z., Manzie C., Burdet E., Kulić D., Oetomo D. & Tan Y. (2024). A biomechanics and energetics dataset of neurotypical adults walking with and without kinematic constraints, Science Date, 11(1), 646.
6. Blickhan, R. (1989). The spring–mass model for running and hopping. J. Biom., 22(11–12), 1217–1227.
7. Cavagna, G.A., Willems, P.A., Legramandi, M.A., & Heglund, N. C. (2002). Pendular energy transduction within the step in human walking. J. Exp. Biol., 205(21), 3413–3422.
8. Cavagna, G.A., Legramandi, M.A., & Peyré-Tartaruga, L.A. (2008). Old men running: mechanical work and elastic bounce. Pro. Roy. Soc. B, 275, 411–418.
9. Chiari, L., Della Croce, U., Leardini, A., & Cappozzo, A. (2005). Human movement analysis using stereophotogrammetry: Part 2 – Ins. err. Gait & Pos., 21(2), 197–211.
10. Derrick, T.R., Dereu, D., & McLean, S.P. (1998). Impacts and kinematic adjustments during running. J. Biom., 31(10), 951–956.
11. Donelan, J.M., Kram, R., & Kuo, A.D. (2002). Mechanical work for step-to-step transitions is a major determinant of the metabolic cost of human walking. J. Exp. Biol., 205(23), 3717–3727.
12. Farley, C.T., & González, O. (1996). Leg stiffness and stride frequency in human running. J. Biom., 29(2), 181–186.
13. Farris, D.J., & Sawicki, G.S. (2012). The mechanics and energetics of human walking and running: a joint level perspective. J. Roy. Soc. Int., 9(66), 110–118.
14. Farris, D.J., Ha, S., & Sawicki, G.S. (2016). Elastic ankle exoskeletons reduce metabolic cost. J. Neuro Engg. Reh., 13, 97.

15. Fukuchi, R.K., Fukuchi, C.A., & Duarte, M. (2017). A public dataset of running biomechanics and the effects of running speed on lower extremity kinematics and kinetics. PeerJ, 5, e3298.
16. Hof, A.L., Gazendam, M.G.J., & Sinke, W.E. (2005). The condition for dynamic stability. J. Biom., 38(1), 1–8.
17. Jiang X., Bíró I., Sárosi J., Fang Y. & Gu Y. (2024) Comparison of ground reaction forces as running speed increases between male and female runners, Front. Bio. Biot., 12, 1378284.
18. Kram, R., & Taylor, C.R. (1990). Energetics of running: a new perspective. Nature, 346(6281), 265–267.
19. Krebbekx G.G.J. Waterval N.F.J., Brehm M.A., Kerkhoffs G.M.M.J., Bramer J.A.M. & Verspoor F.G.M. (2025). Gait biomechanics and energy cost of walking after rotationplasty: A systematic review and meta-analysis compared to above-knee amputation and healthy participants, Cli. Biom., 128, 106626.
20. Luciano F. , Minetti A. E., & Pavei G. (2024), Metabolic cost and mechanical work of walking in a virtual reality emulator, Eur. J. App. Phy., 124, 783–792.
21. McMahon, T.A., & Cheng, G.C. (1990). The mechanics of running: How does stiffness couple with speed? J. Biom., 23(Suppl 1), 65–78.
22. Mercer, J.A., D. Paul; D., Tim R., & Bates, B.T. (2003). Individual Effects of Stride Length and Frequency on Shock Attenuation during Running, Med. & Sci. in Spo. & Ex., 35(2), 307-313.
23. Mercer J.A., Vance J., Hreljac A., & Hamill J. (2002). Relationship between shock attenuation and stride length during running at different velocities, Eur. J. App. Phy., 87, 403-408.
24. Mero, A., Komi, P.V. & Gregor, R.J. (1992). Biomechanics of Sprint Running: A Review, Spo. Med., 13 (6), 376-392.
25. Nilsson, J., & Thorstensson, A. (1989). Ground reaction forces at different speeds of human walking and running. Acta Phy. Sca., 136(2), 217–227.
26. Novacheck T.F., The biomechanics of running. Gait Pos., 1998;7(1):77–95.
27. Orr S., Casler J., Rhoades J., & Leon, P. de. (2022). Effects of walking, running, and skipping under simulated reduced gravity using the NASA Active Response Gravity Offload System (ARGOS), Acta Ast., 197, 115-125.
28. Pavei G., Zamparo P., Fujii N., Otsu T., Numazu N., Minetti A.E., & Monte A. (2019) Comprehensive mechanical power analysis in sprint running acceleration. Sca. J Med. Sci. Spo., 29,1892–1900.
29. Robertson, D.G.E., Caldwell, G.E., Hamill, J., Kamen, G., & Whittlesey, S. (2013). Research methods in biomechanics (2nd ed.). Champaign, IL: Human Kinetics, ISBN: 0-7360-8340-0.
30. Riddick,R.C.,& Kuo, A.D. (2022). Mechanical work accounts for most of the energetic cost in human running. Sci. Rep., 12, 645.
31. Schache, A.G., Blanch, P.D., Dorn, T.W., Brown, N.A.T., Rosemond, D., & Pandy, M.G. (2011). Effect of running speed on lower limb joint kinetics. Med. Sci. Sp. Ex., 43(7), 1260–1271.
32. Seyfarth, A., Geyer, H., Günther, M., & Blickhan, R. (2002). A movement criterion for running. J. Biom., 35(5), 649–655.
33. Tan T., Wouwe T.V., Werling K.F., Liu C.K., Delp S.L., Hicks J.L., & Chaudhari A.S. (2026), GaitDynamics: a generative foundation model for analyzing human walking and running. J. Res. Sq., https://doi.org/10.1038/s41551-025-01565-8.
34. Usherwood, J.R. (2024), The functions of leg muscles, structures and mechanisms in running, Biol. Let., 20, 0260.
35. Willems, P.A. Cavagna, G.A., & Heglund, N.C. (1995). External, internal and total work in human locomotion. J. Exp. Biol., 198(2), 379–393.
36. Winter. D.A. (2009). Biomechanics and motor control of human movement. 4th ed. Hoboken (NJ): John Wiley & Sons.
37. Winter, D.A. (1995). Human balance and posture control during standing and walking. Gait & Posture, 3(4), 193–214.